

A Directional Rouy-Tourin Scheme for Adaptive Matrix-Valued Morphology

Luis Pizarro, Bernhard Burgeth, Michael Breuß, and Joachim Weickert

Mathematical Image Analysis Group
Faculty for Mathematics and Computer Science
Saarland University, Building E11, 66041 Saarbrücken, Germany
{pizarro,burgeth,breuss,weickert}@mia.uni-saarland.de
<http://www.mia.uni-saarland.de>

Abstract. In order to describe anisotropy in image processing models or physical measurements, matrix fields are a suitable choice. In diffusion tensor magnetic resonance imaging (DT-MRI), for example, information about the diffusive properties of water molecules is captured in symmetric positive definite matrices. The corresponding matrix field reflects the structure of the tissue under examination. Recently, morphological partial differential equations (PDEs) for dilation and erosion known for grey scale images have been extended to matrix-valued data.

In this article we consider an adaptive, PDE-driven dilation process for matrix fields. The anisotropic morphological evolution is steered with a matrix constructed from a structure tensor for matrix valued data. An important novel ingredient is a directional variant of the matrix-valued Rouy-Tourin scheme that enables our method to complete or enhance anisotropic structures effectively. Experiments with synthetic and real-world data substantiate the gap-closing and line-completing properties of the proposed method.

1 Introduction

The enhancement and extraction of shape information from image objects is one of the principle tasks of mathematical morphology. Traditionally this task is successfully tackled with morphological operations based on the fundamental dilation process. Dilation and erosion can be realised in a set-theoretic or ordering based framework, see e.g. [17, 21, 18, 22–24], but it may also be implemented within the context of partial differential equations (PDE) [1, 2, 7, 20, 25] and their numerical solution schemes (see [6] as well as the extensive list of literature cited there). On a set-theoretic basis, locally adaptive linear structuring elements whose directions are inferred from a diffused squared gradient field have been introduced for binary images in [26]. The PDE-based approach is conceptually attractive since it allows for digital scalability and even adaptivity of the represented structuring element. This versatility was exploited, for example in [5] to create a adaptive, PDE-based dilation process for grey value images. In [9] the idea of morphological adaptivity has been transferred to the setting of

matrix fields utilising the operator-algebraic framework proposed in [11]. The goal of [9] was to enhance line-like structures in diffusion tensor magnetic resonance imaging (DT-MRI), the main source of matrix fields consisting of positive semidefinite matrices.

In this article we propose a concept for PDE-based adaptive morphology for matrix fields, involving directional derivatives in the formulation of the PDE-based dilation process. In contrast to the work in [9] the numerical realisation employed in this article takes advantage of the accurate calculation of directional derivatives that relies on bi-linear interpolation.

We will start from a scalar adaptive formulation for d -dimensional data u in form of the dilation PDE

$$\partial_t u = \|M(u) \cdot \nabla u\| \quad (1)$$

with a data dependent, symmetric, positive semidefinite $d \times d$ -matrix $M = M(u)$. Let us consider greyvalue images ($d = 2$): Then one has $M = \begin{pmatrix} a & b \\ b & c \end{pmatrix} = \begin{pmatrix} \|(a,b)\| \nu^\top \\ \|(b,c)\| \eta^\top \end{pmatrix}$ with unit vectors $\nu = \frac{1}{\|(a,b)\|} \begin{pmatrix} a \\ b \end{pmatrix}$ and $\eta = \frac{1}{\|(b,c)\|} \begin{pmatrix} b \\ c \end{pmatrix}$. This turns (1) into

$$\partial_t u = \sqrt{(a\partial_x u + b\partial_y u)^2 + (b\partial_x u + c\partial_y u)^2}, \quad (2)$$

$$= \sqrt{\|(a,b)\|^2 (\partial_\nu u)^2 + \|(b,c)\|^2 (\partial_\eta u)^2}. \quad (3)$$

In [9] the partial derivatives $\partial_x u$ and $\partial_y u$ in (2) were approximated with the standard Rouy-Tourin scheme [19] to obtain a directional derivative, which might lead to numerical artifacts. Now, however, we calculate the directional derivatives necessary for the steering process directly by means of equation (3). Hence it is decisive for our approach to implement the directional derivatives $\partial_\nu u$ and $\partial_\eta u$ in (3) via a directional version of the Rouy-Tourin scheme as will be explained in Section 4.

Equation (1) describes a dilation with an ellipsoidal structuring element since an application of the mapping $(x, y)^\top \mapsto M(x, y)^\top$ transforms a sphere centered around the origin into an ellipse. The necessary directional information of the evolving u contained in the matrix M may be derived from the so-called structure tensor. The structure tensor, dating back to [15, 4], allows to extract directional information from an image. It is given by

$$S_\rho(u(x)) := G_\rho * (\nabla u(x) \cdot (\nabla u(x))^\top) = (G_\rho * (\partial_{x_i} u(x) \cdot \partial_{x_j} u(x)))_{i,j=1,\dots,d} \quad (4)$$

Here $G_\rho*$ indicates a convolution with a Gaussian of standard deviation ρ . For more details the reader is referred to [3] and the literature cited there. In [8, 14] Di Zenzo's approach [13] to construct a structure tensor for multi-channel images has been extended to matrix fields yielding a standard structure tensor

$$J_\rho(U(x)) := \sum_{i,j=1}^m S_\rho(U_{i,j}(x)) \quad (5)$$

with matrix entries $U_{i,j}$, $i, j = 1, \dots, m$. This tensor is a special case of the *full structure tensor concept* for matrix fields as proposed in [12]. For our purpose it suffices to use the standard tensor $J_\rho(U(x))$ to infer directional information from matrix fields.

The article is structured as follows: In Section 2 we will briefly give an account of basic notions of matrix analysis needed to establish a matrix-valued PDE for an adaptively steered morphological dilation process. We introduce the steering tensor that guides the dilation process adaptively in Section 3. It is explained how the numerical scheme of Rouy and Tourin is turned into a directional variant that can be used on matrix fields in Section 4. An evaluation of the performance of our approach to adaptive morphology for matrix fields is the subject of Section 5. The remarks in Section 6 conclude this article.

2 Elements of Matrix Analysis

This section provides the essential notions for the formulation of matrix-valued PDEs. For a more detailed exposition the reader is referred to [11].

A matrix field is considered as a mapping $F : \Omega \subset \mathbb{R}^d \rightarrow \text{Sym}_m(\mathbb{R})$ from a d -dimensional image domain into the set of symmetric $m \times m$ -matrices with real entries, $F(x) = (F_{p,q}(x))_{p,q=1,\dots,m}$. The set of positive semi-definite matrices, denoted by $\text{Sym}_m^+(\mathbb{R})$, consists of all symmetric matrices A with $\langle v, Av \rangle := v^\top Av \geq 0$ for $v \in \mathbb{R}^m$. DT-MRI produces matrix fields with this property. Note that at each point x the matrix $F(x)$ of a field of symmetric matrices can be diagonalised yielding $F(x) = V(x)^\top D(x)V(x)$, where $V(x)$ is a orthogonal matrix, while $D(x) = \text{diag}(\lambda_1, \dots, \lambda_m)$ represents a diagonal matrix with the eigenvalues $\lambda_1 \geq \lambda_2 \geq \dots \geq \lambda_m \in \mathbb{R}$ of $F(x)$ as entries.

The extension of a function $h : \mathbb{R} \rightarrow \mathbb{R}$ to $\text{Sym}_m(\mathbb{R})$ is standard [16]: We set $h(U) := V^\top \text{diag}(h(\lambda_1), \dots, h(\lambda_m))V \in \text{Sym}_m^+(\mathbb{R})$. Specifying $h(s) = |s|$, $s \in \mathbb{R}$ as the absolute value function leads to the absolute value $|A| \in \text{Sym}_m^+(\mathbb{R})$ of a matrix A . The *partial derivative* for matrix fields at ω_0 is handled *componentwise*: $\bar{\partial}_\omega U(\omega_0) = (\partial_\omega U_{p,q}(\omega_0))_{p,q}$ where $\bar{\partial}_\omega$ stands for a spatial or temporal derivative. We define the *generalised gradient* $\bar{\nabla}U(x)$ at a voxel $x = (x_1, \dots, x_d)$ by

$$\bar{\nabla}U(x) := (\bar{\partial}_{x_1}U(x), \dots, \bar{\partial}_{x_d}U(x))^\top \quad (6)$$

which is an element of $(\text{Sym}_m(\mathbb{R}))^d$, in close analogy to the scalar setting where $\nabla u(x) \in \mathbb{R}^d$. For (extended) vectors $W \in (\text{Sym}_m(\mathbb{R}))^d$ with matrix components we set $|W|_p := \sqrt[p]{|W_1|^p + \dots + |W_d|^p}$ for $p \in]0, +\infty[$. It results in a positive semidefinite matrix from $\text{Sym}_m^+(\mathbb{R})$, the direct counterpart of a nonnegative real number as the length of a vector in \mathbb{R}^d . Since the product of two symmetric matrices is in general not symmetric we employ the so-called *Jordan product*

$$A \bullet B := \frac{1}{2}(AB + BA). \quad (7)$$

It produces a symmetric matrix, and it is commutative but neither associative nor distributive. In the proposed numerical scheme we will use the maximum

and minimum of two symmetric matrices A, B . In direct analogy with relations known to be valid for real numbers one defines [10]:

$$\max(A, B) = \frac{1}{2}(A + B + |A - B|), \quad \min(A, B) = \frac{1}{2}(A + B - |A - B|), \quad (8)$$

where $|F|$ stands for the absolute value of the matrix F . Now we are in the position to formulate the matrix-valued counterpart of (1) as follows:

$$\bar{\partial}_t U = |\bar{M}(U) \bullet \bar{\nabla} U|_2 \quad (9)$$

with an initial matrix field $F(x) = U(x, 0)$. Here $\bar{M}(U)$ denotes a symmetric $md \times md$ -block matrix with d^2 blocks of size $m \times m$ that is multiplied block-wise with $\bar{\nabla} U$ employing the symmetrised product " \bullet ". Note that $|\cdot|_2$ stands for the length of $\bar{M}(U) \bullet \bar{\nabla} U$ in the matrix valued sense. The construction of $\bar{M}(U)$ is detailed in the next section.

3 Steering Matrix $\bar{M}(U)$ for Matrix Fields

With these notions at our disposal we propose the following construction of the steering matrix \bar{M} in the adaptive dilation process for matrix fields.

First, the directional information is deduced from the standard structure tensor $J_\rho(U)$ in (5); this symmetric $d \times d$ -matrix $J_\rho(U)$ is spectrally decomposed, and the following mapping is applied:

$$H : \begin{cases} \mathbb{R}_+^d \longrightarrow \mathbb{R}^d \\ (\lambda_1, \dots, \lambda_d) \longmapsto \frac{c}{\lambda_1 + \dots + \lambda_d} (\lambda_d, \lambda_{d-1}, \dots, \frac{K}{c} \cdot \lambda_1) \end{cases}, \quad (10)$$

with constants $c, K > 0$. H applied to $J_\rho(U)$ yields the steering matrix M ,

$$M := H(J_\rho(U)).$$

The eigenvalues of $J_\rho(U)$ fulfil $\lambda_1 \geq \dots \geq \lambda_d$. Hence, the ellipsoid associated with the quadratic form of M is flipped, and, depending on the choice of K , more excentric if compared with $J_\rho(U)$. In this way we enforce dilation towards the direction of least contrast, i. e. along structures.

Second, in order to enable a proper matrix-vector-multiplication we enlarge the $d \times d$ -matrix M to a $md \times md$ -matrix \bar{M} by an extension operation utilising the $m \times m$ -identity matrix I_m and the so-called Kronecker product [16]:

$$\bar{M} = M \otimes \begin{pmatrix} I_m & \cdots & I_m \\ \vdots & \ddots & \vdots \\ I_m & \cdots & I_m \end{pmatrix} = \begin{pmatrix} M_{11}I_m & \cdots & M_{1d}I_m \\ \vdots & \ddots & \vdots \\ M_{d1}I_m & \cdots & M_{dd}I_m \end{pmatrix} \quad (11)$$

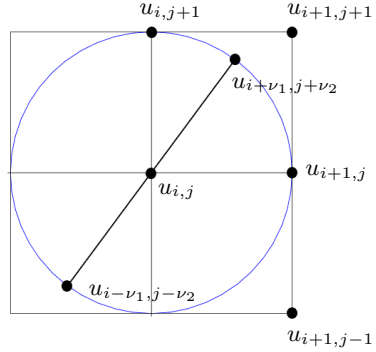
which yields a suitably sized (block-) matrix.

4 Matrix-Valued Directional Numerical Scheme

The first-order finite difference method of *Rouy and Tourin* [19] may be used to solve the scalar PDE (3) in the *isotropic* case with $M = I_d$. Let us denote by $u_{i,j}^n$ the grey value of a scalar 2D image u at the pixel centred in $(ih_x, jh_y) \in \mathbb{R}^2$ at the time-level $n\tau$ of the evolution. Furthermore, we employ standard forward and backward difference operators, i.e., $D_+^x u_{i,j}^n := u_{i+1,j}^n - u_{i,j}^n$ and $D_-^x u_{i,j}^n := u_{i,j}^n - u_{i-1,j}^n$ with spatial grid size h_x, h_y in x - and y -direction, respectively. The Rouy-Tourin method utilises an *upwind approximation* in the pixel (ih_x, jh_y) of the partial derivative u_x (and analogously u_y):

$$u_x \approx \max \left(\frac{1}{h_x} \max(-D_-^x u_{i,j}^n, 0), \frac{1}{h_x} \max(D_+^x u_{i,j}^n, 0) \right). \quad (12)$$

For a unit vector $\nu = (\nu_1, \nu_2)^\top$ the directional derivative $\partial_\nu u$ of u may be approximated by $\partial_\nu u = \langle \nu, \nabla u \rangle = \nu_1 \partial_x u + \nu_2 \partial_y u$. Hence it is close at hand to approximate numerically equation (2) directly. However, this favours mass transport along the directions of the x - and y -axis leading to a poor representation of the directional derivative. Instead we take advantage of equation (3) in this article and propose an alternative involving an interpolated function value $u_{i+\nu_1, j+\nu_2}$ defined by the subsequent bi-linear¹ approximation (13).



$$\begin{aligned} u_{i+\nu_1, j+\nu_2} &= u_{i,j} \cdot (1 - h_x |\nu_1|) \cdot (1 - h_y |\nu_2|) \\ &+ u_{i+\text{sign}(\nu_1), j} \cdot h_x |\nu_1| \cdot (1 - h_y |\nu_2|) \\ &+ u_{i, j+\text{sign}(\nu_2)} \cdot (1 - h_x |\nu_1|) \cdot h_y |\nu_2| \\ &+ u_{i+\text{sign}(\nu_1), j+\text{sign}(\nu_2)} \cdot h_x |\nu_1| \cdot h_y |\nu_2| \end{aligned} \quad (13)$$

Fig. 1. Interpolated image value $u_{i+\nu_1, j+\nu_2}$ with $\sqrt{\nu_1^2 + \nu_2^2} = 1$. It allows for backward and forward finite differences in the direction of $(\nu_1, \nu_2)^\top$.

This leads to forward and backward difference operators in the direction of ν with $\|\nu\| = \|(\nu_1, \nu_2)\| = \sqrt{\nu_1^2 + \nu_2^2} = 1$:

$$D_+^\nu u_{i,j}^n := u_{i+\nu_1, j+\nu_2}^n - u_{i,j}^n \quad \text{and} \quad D_-^\nu u_{i,j}^n := u_{i,j}^n - u_{i-\nu_1, j-\nu_2}^n \quad (14)$$

¹ For the sake of efficiency we use bi-linear interpolation, although higher order alternatives such as bi-cubic or spline interpolation can be employed as well.

and to a direct approximation of the directional derivative

$$\partial_\nu u = u_\nu \approx \max\left(\frac{1}{h} \max(-D_-^\nu u_{i,j}^n, 0), \frac{1}{h} \max(D_+^\nu u_{i,j}^n, 0)\right) \quad (15)$$

where $h := \min(h_x, h_y)$. The extension to higher dimensions poses no problem. Furthermore, the resulting approximation of the directional derivatives is also consistent: Note that bi-linear approximation implies $u_{i+\nu_1, j+\nu_2} = u((i + \nu_1)h_x, (j + \nu_2)h_y) + \mathcal{O}(h_x \cdot h_y)$, and hence

$$\begin{aligned} \frac{1}{h} D_+^\nu u_{i,j} &= \frac{1}{h} (u((i + \nu_1)h_x, (j + \nu_2)h_y) - u(ih_x, jh_y)) + \mathcal{O}(\max(h_x, h_y)) \\ &= u_\nu + \mathcal{O}(\max(h_x, h_y)). \end{aligned} \quad (16)$$

Analogous reasoning applies to $D_-^\nu u_{i,j}$. With the calculus concept presented in Section 2 it is now straightforward to define one-sided directional differences in ν -direction for matrix fields of $m \times m$ -matrices:

$$D_+^\nu U^n(ih_x, jh_y) := U^n((i+\nu_1)h_x, (j+\nu_2)h_y) - U^n(ih_x, jh_y) \in \text{Sym}_m(\mathbb{R}), \quad (17)$$

$$D_-^\nu U^n(ih_x, jh_y) := U^n(ih_x, jh_y) - U^n((i-\nu_1)h_x, (j-\nu_2)h_y) \in \text{Sym}_m(\mathbb{R}). \quad (18)$$

In order to avoid confusion with the subscript notation for matrix components we wrote $U(ih_x, jh_y)$ to indicate the (matrix-) value of the matrix field evaluated at the voxel centred at $(ih_x, jh_y) \in \mathbb{R}^2$. The η -direction is treated accordingly. The notion of supremum and infimum of two matrices – as needed in a matrix variant of Rouy-Tourin – has been provided in Section 2 as well. Hence, having these generalisations at our disposal a directionally adaptive version of the Rouy-Tourin scheme is available now in the setting of matrix fields simply by replacing grey values $u_{i,j}^n$ by matrices $U^n(ih_x, jh_y)$ and utilising the directional derivative approximations.

5 Experiments

Each matrix of the field is represented and visualised as an ellipsoid resulting from the level set of the quadratic form $\{x^\top A^{-2}x = \text{const.} : x \in \mathbb{R}^3\}$ associated with a matrix $A \in \text{Sym}_3^+(\mathbb{R})$. By employing A^{-2} the length of the semi-axes of the ellipsoid correspond directly with the three eigenvalues of the matrix. We apply our PDE-driven adaptive dilation process to synthetic 2D data as well as to real DT-MRI data. For the explicit numerical scheme we used a time step size of 0.1, grid size $h = h_x = h_y = 1$, and $c = 0.01 \cdot K$ in (10).

Figure 2(a) exhibits a 32×32 synthetic matrix field used for testing. It is composed of two interrupted diagonal stripes with different thickness, built from cigar-shaped ellipsoids of equal size but different orientation. The lines intersect the x -axis with an angle of about -63 degrees. Figure 2(b) shows the result of applying the proposed adaptive dilation process using a directional Rouy-Tourin (D-RT) scheme (9). Note that the direction and amount of anisotropic dilation

does not depend on the orientation of the ellipsoids, but on the orientation and strength of the structural conformations.

Figure 2(c) displays another 32×32 testing image, namely a spiral-like field where large portions of the spiral have been removed. Figures 2(d), 2(e) and 2(f) depict the results of applying isotropic dilation [10], adaptive dilation with the classical Rouy-Tourin (RT) scheme [9], and the proposed adaptive dilation employing a directional Rouy-Tourin (D-RT) scheme (9). Comparatively, classical isotropic dilation requires much more time to fill in the missing ellipsoids and it also broadens the structures in all directions. Adaptive dilation with the RT scheme as in [9] does close the gaps in an anisotropic manner. However, numerous artifacts appear due to the numerical scheme bias to the coordinate axes. This problem is successfully solved in our PDE-based adaptive dilation process by utilising a D-RT scheme for approximating the partial derivatives. Evidently, relying on the D-RT scheme is much more accurate for longer dilation times.

We also tested the proposed method on a real DT-MRI data set of a human head consisting of a $128 \times 128 \times 38$ -field of positive definite matrices. Figure 3(a) shows the lateral ventricles in a 40×55 2D section. Adaptive dilation with the classical RT scheme [9] and the proposed adaptive dilation process with a D-RT scheme (9) are shown in Figures 3(b) and 3(c), respectively. For a better comparison we scale-up these images around the *genu* area in Figures 3(d)-(g), including isotropic dilation [10] in Fig.3(e). Due to measurement errors the fibre tracts are interrupted in the original data. These holes are quickly and anisotropically filled by our directional-adaptive dilation process while enhancing slightly the directional structure of the fibres and preserving the shape of the ventricles. The adaptive dilation process with the classical RT scheme presented in [9] is affected by numerical artifacts and isotropic dilation [10] is too dissipative.

6 Conclusion

In this article we have presented a method for an adaptive, PDE-based dilation process in the setting of matrix fields. The evolution governed by a matrix-valued PDE is guided by a steering tensor. In order to enable proper directional steering we extended the classical Rouy-Tourin method in two ways: First, turning it into a directional Rouy-Tourin scheme based on directional finite differences via interpolation. Second, by means of matrix calculus, extending this directional scheme to matrix fields solving the matrix valued adaptive dilation PDE. Preliminary tests on synthetic and real DT-MRI data reveal a good performance of the method when it comes to filling in of missing data and segmentation of image structures involving directional information. As such the proposed approach may have its merits, for example, as a preprocessing step for fiber tracking algorithms.

Clearly, it is within our reach to formulate the anisotropic counterparts of other morphological operations such as erosion, opening, closing, top hats, gradients etc., which can be employed in more advanced image processing tasks for tensor fields, e.g. filtering and segmentation. In addition, the extension to the 3D setting is straightforward.

Acknowledgements. We gratefully acknowledge partial funding by the *Deutscher Akademischer Austauschdienst* (DAAD), grant A/05/21715.

DT-MRI data set by courtesy of Anna Vilanova i Bartoli, Eindhoven University of Technology.

References

1. L. Alvarez, F. Guichard, P.-L. Lions, and J.-M. Morel. Axioms and fundamental equations in image processing. *Archive for Rational Mechanics and Analysis*, 123:199–257, 1993.
2. A. B. Arehart, L. Vincent, and B. B. Kimia. Mathematical morphology: The Hamilton–Jacobi connection. In *Proc. Fourth International Conference on Computer Vision*, pages 215–219, Berlin, May 1993. IEEE Computer Society Press.
3. J. Bigün. *Vision with Direction*. Springer, Berlin, 2006.
4. J. Bigün, G. H. Granlund, and J. Wiklund. Multidimensional orientation estimation with applications to texture analysis and optical flow. *IEEE Transactions on Pattern Analysis and Machine Intelligence*, 13(8):775–790, August 1991.
5. M. Breuß, B. Burgeth, and J. Weickert. Anisotropic continuous-scale morphology. In J. Martí, J. M. Benedí, A. M. Mendonça, and J. Serrat, editors, *Pattern Recognition and Image Analysis*, volume 4478 of *Lecture Notes in Computer Science*, pages 515–522. Springer, Berlin, 2007.
6. M. Breuß and J. Weickert. A shock-capturing algorithm for the differential equations of dilation and erosion. *Journal of Mathematical Imaging and Vision*, 25(2):187–201, September 2006.
7. R. W. Brockett and P. Maragos. Evolution equations for continuous-scale morphological filtering. *IEEE Transactions on Signal Processing*, 42:3377–3386, 1994.
8. T. Brox, J. Weickert, B. Burgeth, and P. Mrázek. Nonlinear structure tensors. *Image and Vision Computing*, 24(1):41–55, January 2006.
9. B. Burgeth, M. Breuß, L. Pizarro, and J. Weickert. PDE-driven adaptive morphology for matrix fields. In *Proc. Second International Conference on Scale Space and Variational Methods in Computer Vision*. 2009. Accepted for publication.
10. B. Burgeth, A. Bruhn, S. Didas, J. Weickert, and M. Welk. Morphology for matrix-data: Ordering versus PDE-based approach. *Image and Vision Computing*, 25(4):496–511, 2007.
11. B. Burgeth, S. Didas, L. Florack, and J. Weickert. A generic approach to diffusion filtering of matrix-fields. *Computing*, 81:179–197, 2007.
12. B. Burgeth, S. Didas, and J. Weickert. A general structure tensor concept and coherence-enhancing diffusion filtering for matrix fields. Technical Report 197, Department of Mathematics, Saarland University, Saarbrücken, Germany, July 2007. to appear in D. Laidlaw and J. Weickert (Eds.): *Visualization and Processing of Tensor Fields*, Springer, 2009.
13. S. Di Zenzo. A note on the gradient of a multi-image. *Computer Vision, Graphics and Image Processing*, 33:116–125, 1986.
14. C. Feddern, J. Weickert, B. Burgeth, and M. Welk. Curvature-driven PDE methods for matrix-valued images. *International Journal of Computer Vision*, 69(1):91–103, August 2006.
15. W. Förstner and E. Gülch. A fast operator for detection and precise location of distinct points, corners and centres of circular features. In *Proc. ISPRS Intercommission Conference on Fast Processing of Photogrammetric Data*, pages 281–305, Interlaken, Switzerland, June 1987.

16. R. A. Horn and C. R. Johnson. *Matrix Analysis*. Cambridge University Press, Cambridge, UK, 1990.
17. G. Matheron. *Éléments pour une théorie des milieux poreux*. Masson, Paris, 1967.
18. G. Matheron. *Random Sets and Integral Geometry*. Wiley, New York, 1975.
19. E. Rouy and A. Tourin. A viscosity solutions approach to shape-from-shading. *SIAM Journal on Numerical Analysis*, 29:867–884, 1992.
20. G. Sapiro, R. Kimmel, D. Shaked, B. B. Kimia, and A. M. Bruckstein. Implementing continuous-scale morphology via curve evolution. *Pattern Recognition*, 26:1363–1372, 1993.
21. J. Serra. *Echantillonnage et estimation des phénomènes de transition minier*. PhD thesis, University of Nancy, France, 1967.
22. J. Serra. *Image Analysis and Mathematical Morphology*, volume 1. Academic Press, London, 1982.
23. J. Serra. *Image Analysis and Mathematical Morphology*, volume 2. Academic Press, London, 1988.
24. P. Soille. *Morphological Image Analysis*. Springer, Berlin, second edition, 2003.
25. R. van den Boomgaard. *Mathematical Morphology: Extensions Towards Computer Vision*. PhD thesis, University of Amsterdam, The Netherlands, 1992.
26. R. Verdú-Monedero and J. Angulo. Spatially-variant directional mathematical morphology operators based on a diffused average squared gradient field. In J. Blanc-Talon et al., editor, *Advanced Concepts for Intelligent Vision Systems*, volume 5259 of *Lecture Notes in Computer Science*, pages 542–553, Berlin, 2008. Springer.

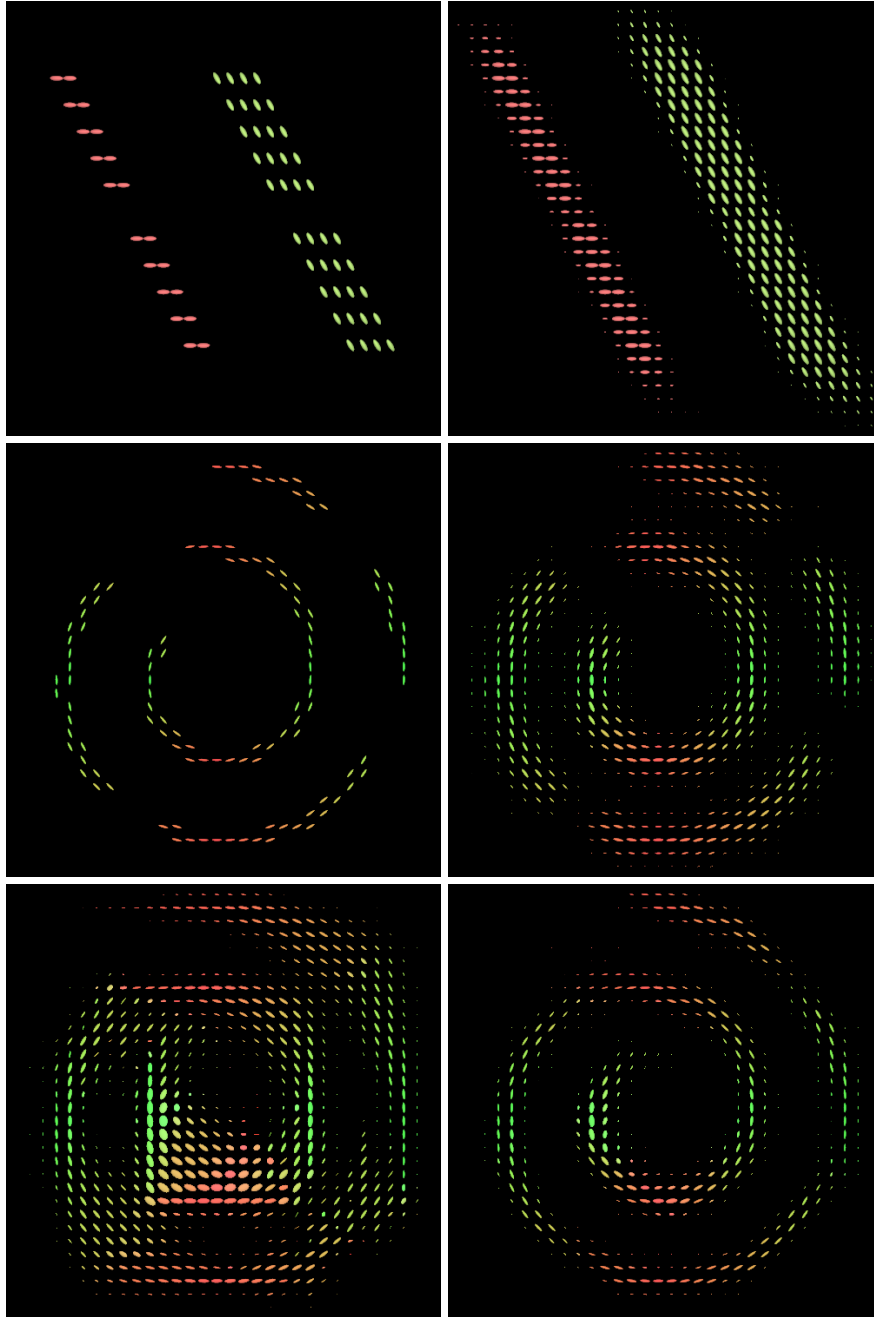


Fig. 2. Synthetic data sets. **(a) Top left:** Ellipsoids in line-like arrangement. **(b) Top right:** Proposed adaptive dilation with D-RT scheme; $K = 20, \rho = 4, t = 1$. **(c) Middle left:** Ellipsoids in spiral arrangement. **(d) Middle right:** Isotropic dilation; $t = 1$. **(e) Bottom left:** Adaptive dilation with RT scheme; $K = 20, \rho = 2, t = 1$. **(f) Bottom right:** Proposed adaptive dilation with D-RT scheme; $K = 20, \rho = 2, t = 1$.

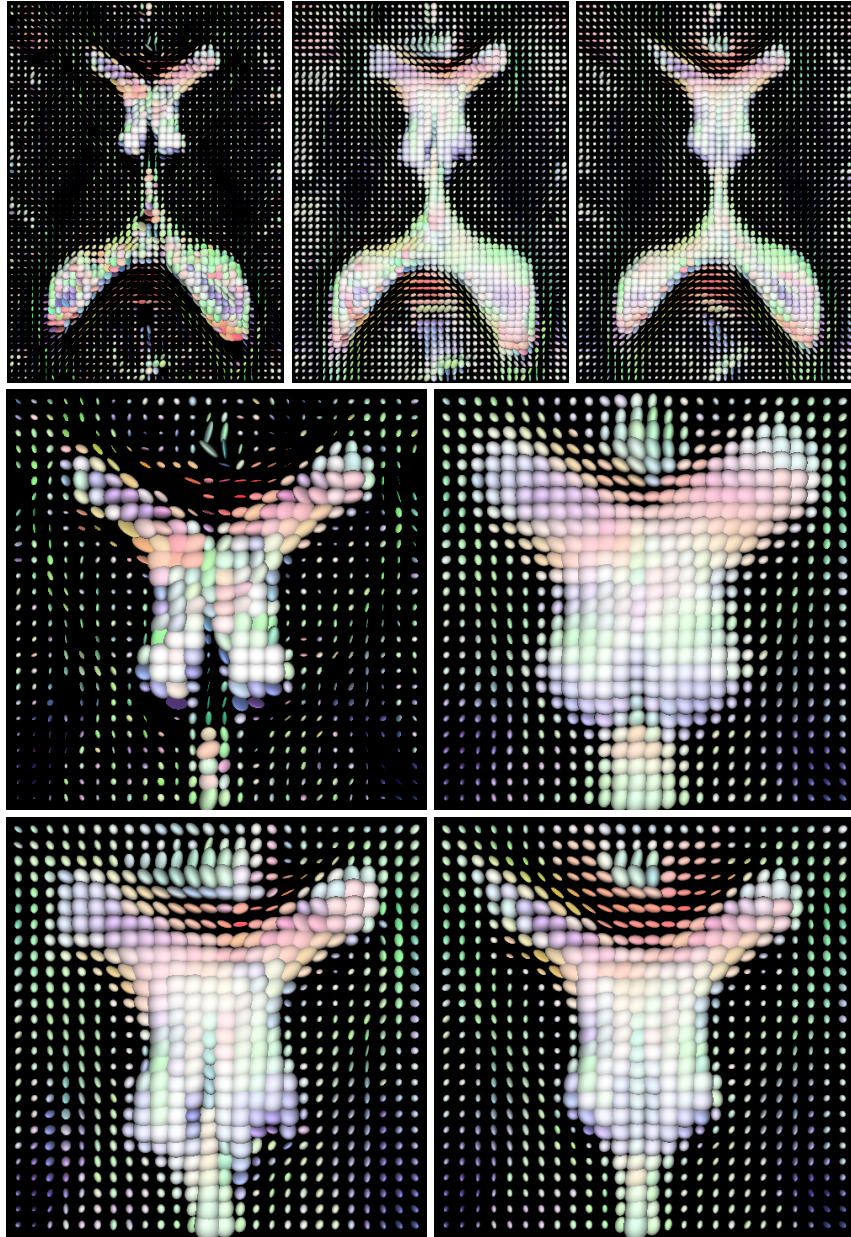


Fig. 3. Real data, 2D-slice of a 3D DT-MRI matrix field, and enlarged regions. **(a) Top left:** Original data set. **(b) Top center:** Adaptive dilation with RT scheme; $K = 10, \rho = 1, t = 1.5$. **(c) Top right:** Proposed adaptive dilation with D-RT scheme; $K = 10, \rho = 1, t = 1.5$. **(d) Middle left:** Zoomed original data set. **(e) Middle right:** Zoomed isotropic dilation after $t = 1.5$. **(f) Bottom left:** Zoomed adaptive dilation with RT scheme. **(g) Bottom right:** Zoomed adaptive dilation with D-RT scheme.